Integrability of Non-KAM Hamiltonians

A. Salat
Max-Planck-Institut für Plasmaphysik, EURATOM Association, Garching

Z. Naturforsch. **39 a**, 830–841 (1984); received June 30, 1984

The integrability of Hamiltonians of the type $H(P_1, P_2, Q_1, Q_2) = \sum_{i=1,2} P_i \cdot G_i(Q_1, Q_2)$, G_i 2π-periodic in Q_1, Q_2, is investigated numerically and analytically. With $G_i = \omega_i + F_i(Q_1, Q_2)$ and $H_0 = \sum_{i=1,2} \omega_i P_i$, the unperturbed frequencies $\omega_i = \partial H_0/\partial P_i$ are independent of the momenta, and KAM theory cannot be applied. Surface of section plots and Fourier analysis of orbits reveal that "most" Hamiltonians are integrable. Possibly non-integrable Hamiltonians do not show "island plus ergodic region" structure but sequences which tend towards infinity. No theory is available to distinguish completely the classes of integrable and non-integrable functions $G_i(Q_1, Q_2)$. In such a theory the problem of "small denominators" would play an essential role just as in KAM theory.

1. Introduction

A Hamiltonian system

$$\dot{p}_i = -\frac{\partial H}{\partial q_i}, \quad \dot{q}_i = \frac{\partial H}{\partial p_i}, \quad i = 1, 2, \ldots, n, \tag{1.1}$$

is called integrable if apart from $H(p_1, \ldots, p_n, q_1, \ldots, q_n)$, $n-1$ analytic single-valued functions $I_i(p_1, \ldots, p_n, q_1, \ldots, q_n)$ exist, $i = 1, 2, \ldots, n-1$, which are constants of the motion, i.e. $\dot{I}_i = 0$. In addition, they have to be linearly independent and in involution with each other, $[I_i, I_k] = 0$. They should also be solvable for $p_1, \ldots, p_n$ [1]. The motion of integrable systems proceeds on nested n-dimensional tori in phase space and does not exhibit the chaotic behaviour familiar from non-integrable Hamiltonian systems [2]. In order to understand the qualitative nature of the motion of a Hamiltonian system, it is therefore important to know whether it is integrable or not.

If an integrable Hamiltonian H_0 is slightly perturbed,

$$H = H_0 + \varepsilon H_1; \quad |\varepsilon| \ll 1, \tag{1.2}$$

the theory of Kolmogorov, Arnold and Moser (KAM) [3] ensures that a large measure of phase space tori does survive. Two conditions, however, related to the fundamental frequencies ω_i, $i = 1, \ldots, n$, of the unperturbed system,

$$\omega_i = \frac{\partial H_0(P_1, \ldots, P_n)}{\partial P_i}, \tag{1.3}$$

have to be satisfied: a) the frequencies ω_i have to be sufficiently irrational, see [2], [3], and b) they have to be functions of the amplitude:

$$\det\left(\frac{\partial \omega_i}{\partial P_j}\right) \equiv \det\left(\frac{\partial^2 H_0(P_1, \ldots, P_n)}{\partial P_j \, \partial P_i}\right) \neq 0. \tag{1.4}$$

These conditions are formulated in terms of action and angle variables P_i, Q_i of the unperturbed Hamiltonian

$$H_0(p_1, \ldots, p_n, q_1, \ldots, q_n) = H_0(P_1, \ldots, P_n).$$

All p_i, q_i are 2π-periodic functions of $Q_1, \ldots, Q_n$. (Instead of condition (1.4) there exists an alternative condition [3] which, however, is equivalent for the present purpose.)

Condition b) excludes a class of Hamiltonians from KAM theory which at first glance might seem to be trivial but which in fact are not, namely those linear in P_i,

$$H = \sum_{i=1,n} P_i \, G_i(Q_1, \ldots, Q_n), \tag{1.5}$$

where the G_i are arbitrary functions, 2π-periodic in each argument. In order to compare whith KAM theory, we split each G_i into an "unperturbed" part, namely an arbitrary constant ω_i and a "perturbation" F_i:

$$G_i = \omega_i + F_i(Q_1, \ldots, Q_n). \tag{1.6}$$

It is useful to assume that $\langle F_i \rangle = 0$, where $\langle \ldots \rangle$ corresponds to averaging with respect to all Q_i. The

0340-4811 / 84 / 0900-0830 $ 01.30/0. – Please order a reprint rather than making your own copy.

"unperturbed" Hamiltonian is taken to be

$$H_0 = \sum_{i=1,n} \omega_i P_i. \tag{1.7}$$

As the notation indicates, P_i and Q_i are automatically action and angle variables for H_0.

With H_0 as defined above, condition (1.4) is violated, and KAM theory does not apply. The purpose of this paper is to obtain some numerical and analytical results on the integrability of such Hamiltonians in the case $n = 2$.

In Sect. 2 we present Poincaré surface of section maps, both for randomly chosen and specifically selected pairs of functions $F_i(Q_1, Q_2)$, $i = 1, 2$. In Sect. 3 we discuss some of the difficulties involved in the analytic treatment of integrability. Section 4 contains a summary and conclusions.

One might think that Hamiltonians (1.5) could be transformed canonically in such a way that some nonlinear $\hat{H}_0$ might be identified. In Appendix A it is shown that this is not the case. Hamiltonians (1.5) are generic.

Hamiltonians of the present type with $n = 3$ occur in plasma physics, in the domain of wave propagation in toroidal configurations [4, 5]. They also occur in solid state physics [11].

2. Numerical investigation

The equations of motion from Hamiltonian (1.5) in the case $n = 2$ are

$$\dot{Q}_i = G_i(Q_1, Q_2), \tag{2.1}$$

$$\dot{P}_i = -\sum_{j=1,2} P_j G_{ij}(Q_1, Q_2) \tag{2.2}$$

for $i = 1, 2$ where

$$G_{ij} = \partial G_i / \partial Q_j = \partial F_i / \partial Q_j. \tag{2.3}$$

The flow (2.1) in (Q_1, Q_2) space may be studied independently of (2.2). There are many topological types of solutions for $Q_2(Q_1)$. Figures 1–7 show some typical cases. While it is not the purpose here to study flows in Q_1, Q_2 space in detail, some topological classification is need below when (2.2) for the momenta is solved and the orbits $Q_i(t)$ enter into the coefficients. In Figs. 1–7 Q_1 and Q_2 are plotted modulo 2π. One starting point only is used throughout in all figures. $\omega_1 = 1$ is kept fixed without loss of generality.

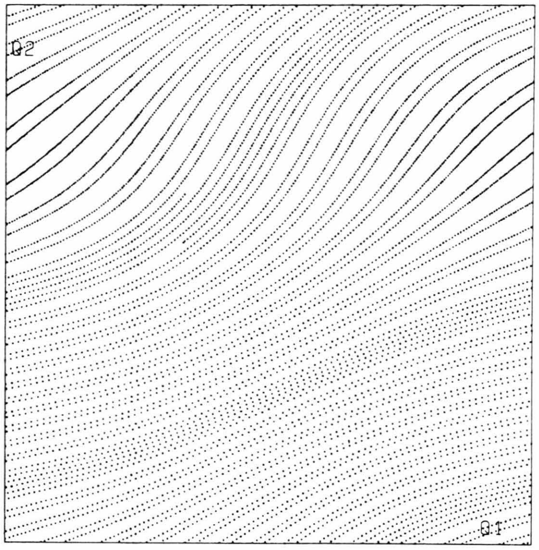

Fig. 1. Orbit $Q_2(Q_1)$ in subspace, case H1; $A_1 = 0.6$, $A_2 = 0.3$; $\omega_2 = 0.521111$.
$F_1 = A_1 \times \sin(Q_2)$;
$F_2 = 2.0 \times A_2 \times (SQRT(1.0 + 0.6 \times \sin(B_2 + Q_1)) - 0.97523$.

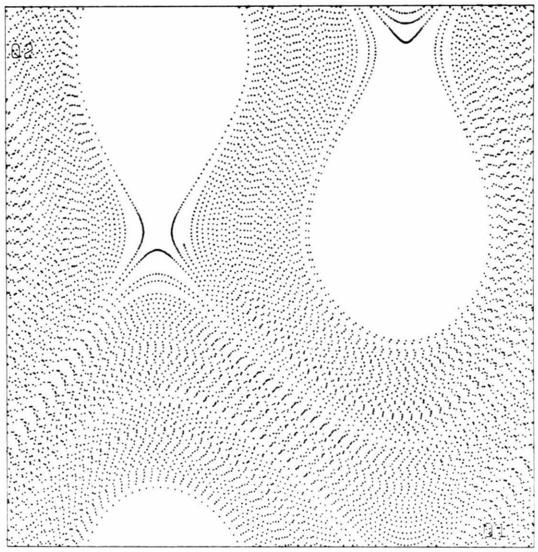

Fig. 2. $Q_2(Q_1)$, case H1; $A_1 = 2.0$, $A_2 = -5.0$; $\omega_2 = 0.521111$.
$F_1 = A_1 \times \sin(Q_2)$;
$F_2 = 2.0 \times A_2 \times (SQRT(1.0 + 0.6 \times \sin(B_2 + Q_1)) - 0.97523$.

Two classes of G_1, G_2 can be distinguished: I) div $\boldsymbol{G} = G_{11} + G_{22} \equiv 0$; the flow in $\boldsymbol{Q}$ space is incompressible, and II) div $\boldsymbol{G} \equiv 0$; the flow has sources and sinks.

In class I, with ω_2/ω_1 "irrational" (see below) the region $0 \leqq Q_i \leqq 2\pi$, $i = 1, 2$ is covered ergodically,

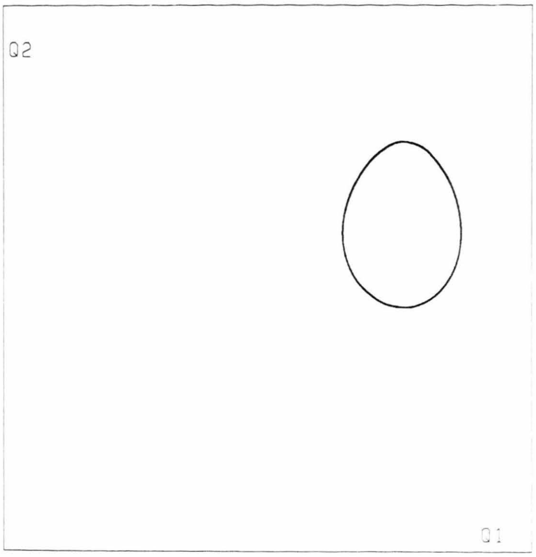

Fig. 3. $Q_2(Q_1)$, case H1; $A_1 = 2.0$, $A_2 = -5.0$; $\omega_2 = 0.521111$; with different starting point to that in Figure 2.
$F_1 = A_1 \times \sin(Q_2)$;
$F_2 = 2.0 \times A_2 \times (SQRT(1.0 + 0.6 \times \sin(B_2 + Q_1)) - 0.97523)$.

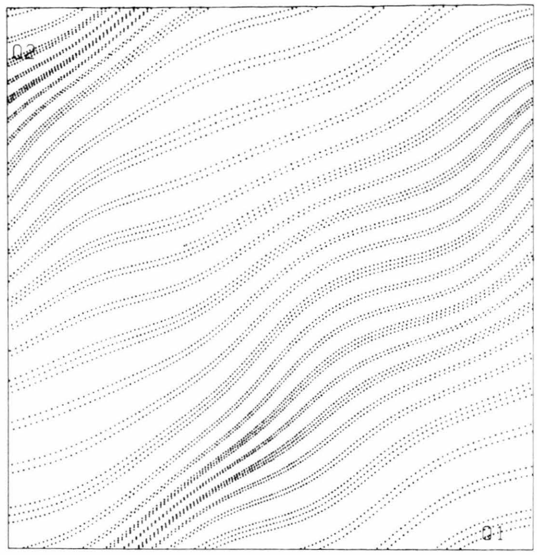

Fig. 5. $Q_2(Q_1)$, case H2; $A_1 = 0.5$, $A_2 = 0.3$; $\omega_2 = 0.521111$.
$F_1 = A_1 \times \cos(Q_1) \times \sin(Q_2)$;
$F_2 = A_2 \times \cos(2 \times Q_1) \times \sin(B_2 + Q_2)$.

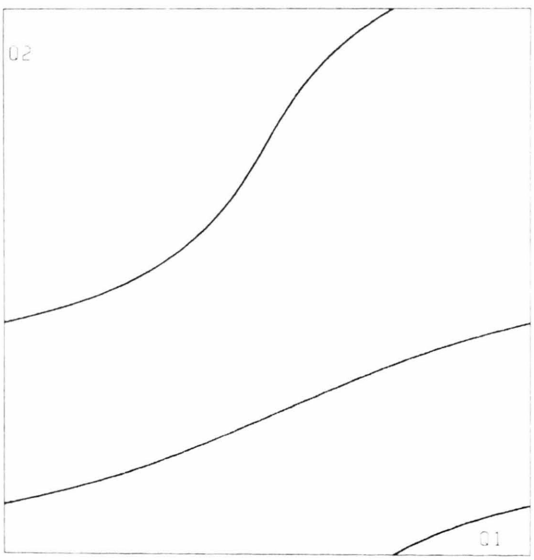

Fig. 4. $Q_2(Q_1)$, case H1; $A_1 = 0.6$, $A_2 = 0.3$; $\omega_2 = 0.5$.
$F_1 = A_1 \times \sin(Q_2)$;
$F_2 = 2.0 \times A_2 \times (SQRT(1.0 + 0.6 \times \sin(B_2 + Q_1)) - 0.97523)$.

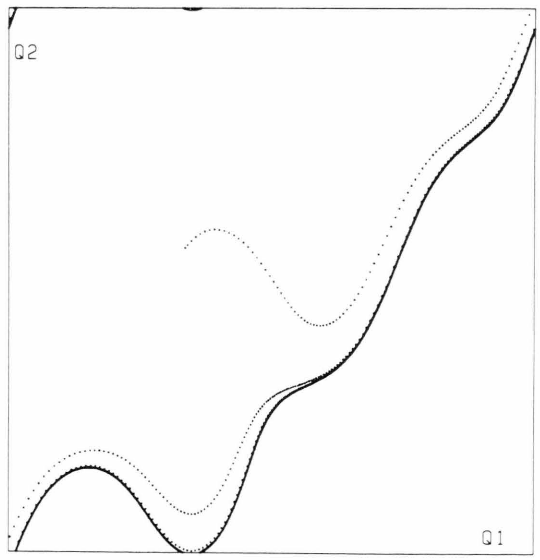

Fig. 6. $Q_2(Q_1)$, case H2; $A_1 = 0.5$, $A_2 = -2.0$; $\omega_2 = 0.521111$; line attractor.
$F_1 = A_1 \times \cos(Q_1) \times \sin(Q_2)$;
$F_2 = A_2 \times \cos(2 \times Q_1) \times \sin(B_2 + Q_2)$.

see Fig. 1, provided that at least one "perturbation" F_i is "small". Here "small" is defined by $|F_i| < |\omega_i|$, so that G_i does not change sign along the orbit. When both "perturbations" are large part of the area may still be filled ergodically, see Fig. 2, while a closed curve results, Fig. 3, if the initial values are chosen in the complement of the ergodic region. For ω_2/ω_1 rational there results a periodic curve, see Fig. 4, or, provided that both "perturbations" are large and the initial values properly chosen, a closed curve as in Fig. 3.

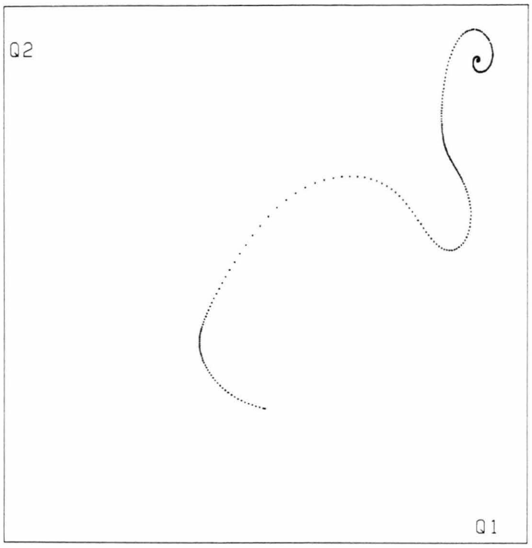

Fig. 7. $Q_2(Q_1)$, case H2; $A_1 = 2.0$, $A_2 = 2.0$; $\omega_2 = 0.521111$; point attractor.
$F_1 = A_1 \times \cos(Q_1) \times \sin(Q_2)$;
$F_2 = A_2 \times \cos(2 \times Q_1) \times \sin(B_2 + Q_2)$.

The functions $F_i(Q_1, Q_2)$ used throughout in Figs. 1–4 are:

$$F_1 = A_2 \sin Q_2,$$

$$F_2 = 2A_2(\sqrt{1 + 0.6 \sin(B_2 + Q_1)} - 0.97523),$$

case H1 for later reference. While the amplitudes A_1, A_2 are indicated in the figures the phases B_1 (see below) and B_2 are kept constant and chosen as 1.23 and 4.56, respectively, throughout the paper. Similarly, $(Q_{10}, Q_{20}) = (0.34, 0.56) \cdot 2\pi$ in all figures except in Figs. 3 and 7, where $(Q_{10}, Q_{20}) = (0.75, 0.75) \cdot 2\pi$ and $(0.50, 0.25) \cdot 2\pi$, respectively.

In class II, div $\boldsymbol{G} \not\equiv 0$, the 2π-square may also be covered ergodically. This is usually found to happen for small "perturbations", see Figure 5. For large "perturbations" all orbits may be attracted to the point(s) where $G_i = 0$ simultaneously for $i = 1, 2$, see the end of the spiral in Figure 7. Furthermore with intermediate amplitudes, all orbits may be attracted to a periodic line attractor, see Figure 6. Situations where all orbits are periodic and closed also exist as evidenced by simple analytic examples. The ratio ω_2/ω_1 is then a function of the amplitudes of F_1 and F_2.

In Figs. 5–7 there is $F_1 = A_1 \cos Q_1 \cdot \sin Q_2$ and $F_2 = A_2 \cos 2Q_1 \cdot \sin(B_2 + Q_2)$, case H2.

After these preliminaries we return to the full system of (2.1), (2.2). In order to study integrability, the surface of section technique is applied: if apart from H a further invariant $I(P_1, P_2, Q_1, Q_2)$ exists, single-valued and 2π-periodic in Q_1, Q_2, then the motion proceeds on a two-dimensional torus surface. At the cut Q_1 modulo $2\pi = Q_{10} =$ const P_1 and P_2 are periodic functions of Q_2, and analogously at the cut Q_2 modulo $2\pi = Q_{20} =$ const. If the surface of section plots, on the other hand do not yield curves but a two-dimensional distribution of points the existence of the above-mentioned invariants is disproved.

The system of (2.1), (2.2) is studied as follows. A pair of functional relationships $F_i(Q_1, Q_2)$, $i = 1, 2$ is chosen. They contain some amplitude and phase constants $A_1, A_2, \ldots, B_1, B_2, \ldots$, which together with the ratio ω_2/ω_1 have to be fixed. Initial values $P_{10}, P_{20}, Q_{10}, Q_{20}$ are also selected. A numerical integration routine is applied long enough for a sufficiently clear picture of the surface of section cut to be obtained. This procedure is repeated for different parameters and different functions F_i.

Equations (2.2) are linear in P_1, P_2. It suffices therefore to vary the initial direction of $\boldsymbol{P} = \boldsymbol{P}_0 = (P_{10}, P_{20})$, with $|\boldsymbol{P}_0| = 1$. With $P_{10}/P_{20} = \operatorname{tg} \alpha$, a particular direction α_0 is defined by

$$\operatorname{tg} \alpha_0 = -\frac{G_2(Q_{10}, Q_{20})}{G_1(Q_{10}, Q_{20})} \tag{2.4}$$

because $H = 0$ for $\alpha = \alpha_0$. In the figures $\Delta\alpha = \alpha_0 - \alpha$ is indicated. It turns out that the most "non-trivial" figures are usually obtained for $\Delta\alpha = \pm 0.5\pi$. See also Sect. 3 below.

It is advantageous to use Q_1 or Q_2 instead of t as the independent parameter in the numerical treatment because no interpolation is required to reach the cuts at Q_1 or Q_2, modulo $2\pi =$ const exactly. Cases where *both* G_1 and G_2 change sign during the evolution have, however, to be excluded then because $\mathrm{d}Q_1/\mathrm{d}t = 0$ and $\mathrm{d}Q_2/\mathrm{d}t = 0$ at those points, respectively.

The essence of the numerical solutions of the combined system of (2.1), (2.2) is contained in the surface of section plots, Figures 8–17. They are representative of the numerous cases studied. Figures 8–15 show regular, sometimes rather involved closed curves. Figure 17 shows a finite number of periodically recurring points, and Fig. 16 presents a sequence of points which tend towards infinity. No case with a two-dimensional distribution of points was ever observed. All Hamiltonians studied were

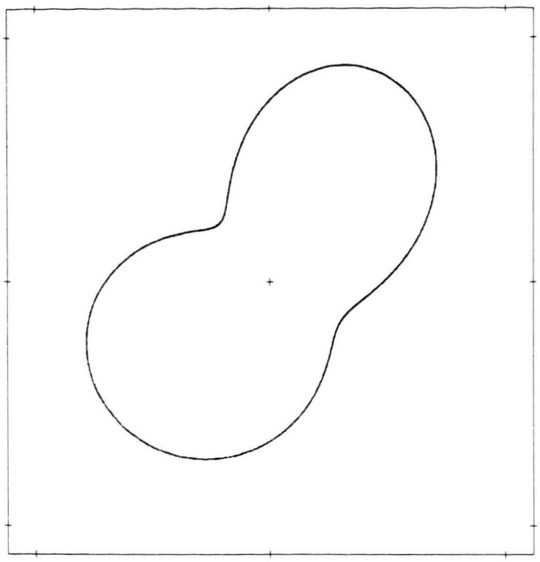

Fig. 8. Surface of section $P_1(Q_2)$ at Q_1 mod $2\pi =$ const, case H1; $A_1 = 0.3$, $A_2 = 0.2$, $\Delta\alpha = 0.5\pi$; $\omega_2 = 0.521111$.
$F_1 = A_1 \times \sin(Q_2)$;
$F_2 = 2.0 \times A_2 \times (SQRT(1.0 + 0.6 \times \sin(B_2 + Q_1)) - 0.97523)$.

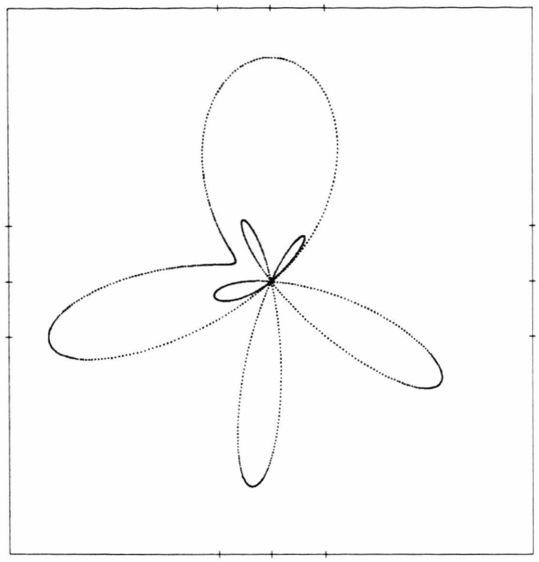

Fig. 10. $P_1(Q_2)$, case H3; $A_1 = 0.5$, $A_2 = 1.0$, $\Delta\alpha = 0.3\pi$; $\omega_2 = 0.521111$.
$F_1 = A_1 \times \sin(Q_2)$;
$F_2 = A_2 \times \sin(B_2 + 2 \times Q_1)$.

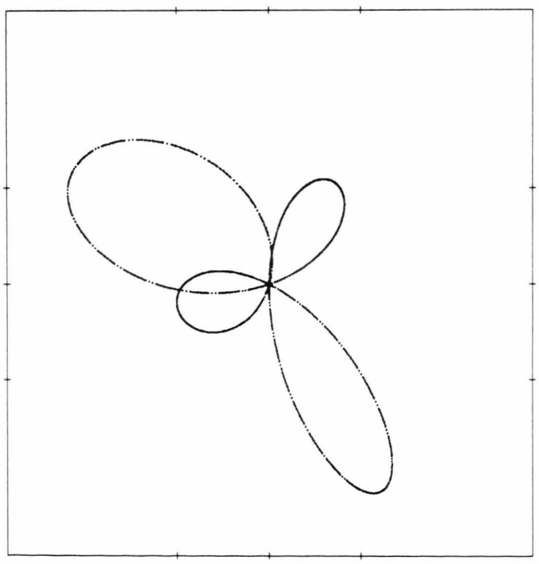

Fig. 9. $P_1(Q_2)$, case H1; $A_1 = 0.5$, $A_2 = 0.5$, $\Delta\alpha = 0.3\pi$; $\omega_2 = 0.521111$.
$F_1 = A_1 \times \sin(Q_2)$;
$F_2 = 2.0 \times A_2 \times (SQRT(1.0 + 0.6 \times \sin(B_2 + Q_1)) - 0.97523)$.

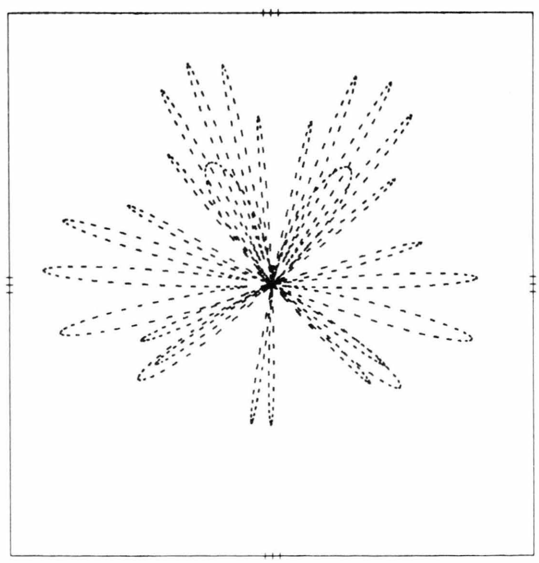

Fig. 11. $P_1(Q_2)$, case H3; $A_1 = 0.8$, $A_2 = 1.0$, $\Delta\alpha = 0.5\pi$; $\omega_2 = 0.521111$.
$F_1 = A_1 \times \sin(Q_2)$;
$F_2 = A_2 \times \sin(B_2 + 2 \times Q_1)$.

therefore integrable, on the graphical scale, or could not be categorized with respect to integrability with the surface of section plots alone.

In the figures $P_1(Q_2)$, in polar coordinates, is plotted for Q_1 modulo $2\pi = Q_{10} =$ const. The unit length is marked on the boundaries. For zero "perturbation", $F_1 = F_2 = 0$, the figures would be unit circles, provided that ω_2/ω_1 is irrational – corresponding to ergodic $Q_2(Q_1)$ flow. For slight "perturbations" the circles are somewhat deformed, see Figs. 8 and 12, 13, with the underlying flow still being ergodic. For larger max $|F_1|$, max $|F_2|$ the

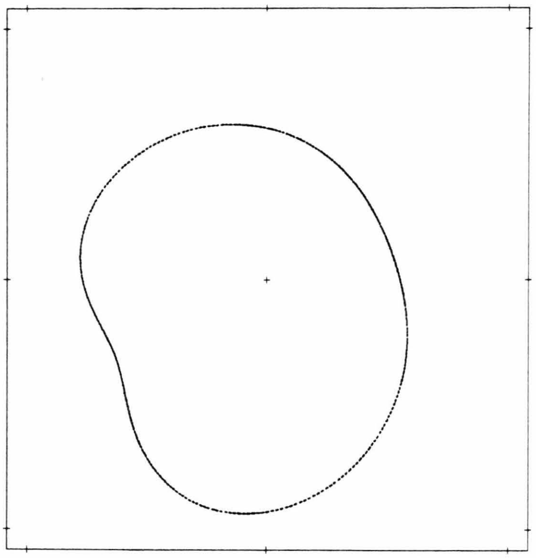

Fig. 12. $P_1(Q_2)$, case H2; $A_1 = 0.3$, $A_2 = 0.2$, $\Delta\alpha = -0.3\,\pi$; $\omega_2 = 0.521111$.
$F_1 = A_1 \times \cos(Q_1) \times \sin(Q_2)$;
$F_2 = A_2 \times \cos(2 \times Q_1) \times \sin(B_2 + Q_2))^2$

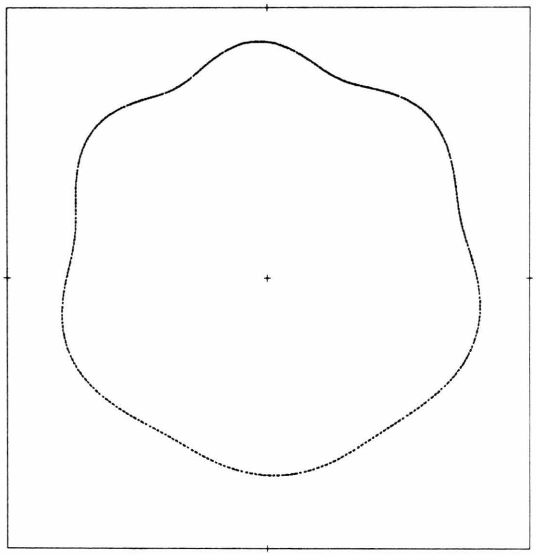

Fig. 13. $P_1(Q_2)$, case H4; $A_1 = -0.95$, $A_2 = 0.3$, $\Delta\alpha = -0.29\,\pi$; $\omega_2 = 0.521111$.
$F_1 = 2.0 \times SQRT(2.0 + \sin(Q_1) + A_1 \times \sin(Q_2))$;
$F_2 = 0.5 \times A_2 \times (\sin(B_1 + Q_1) + 0.6 \times \sin(B_2 + Q_2)^2$

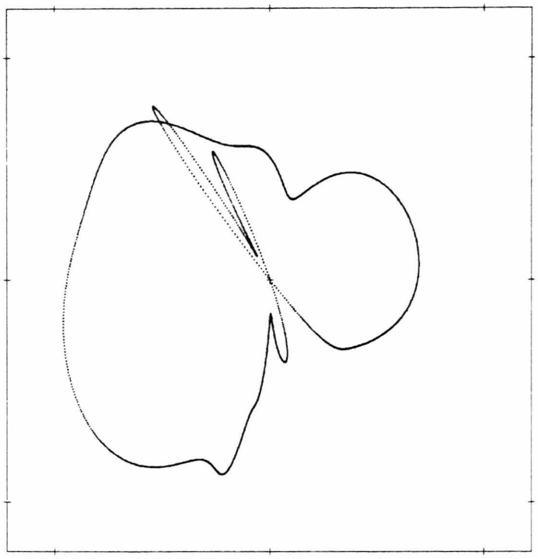

Fig. 14. $P_1(Q_2)$, case H4; $A_1 = 0.3$, $A_2 = -6.0$, $\Delta\alpha = -0.26\,\pi$; $\omega_2 = 0.521111$.
$F_1 = 2.0 \times SQRT(2.0 + \sin(Q_1) + A_1 \times \sin(Q_2))$;
$F_2 = 0.5 \times A_2 \times (\sin(B_1 + Q_1) + 0.6 \times \sin(B_2 + Q_2))^2$

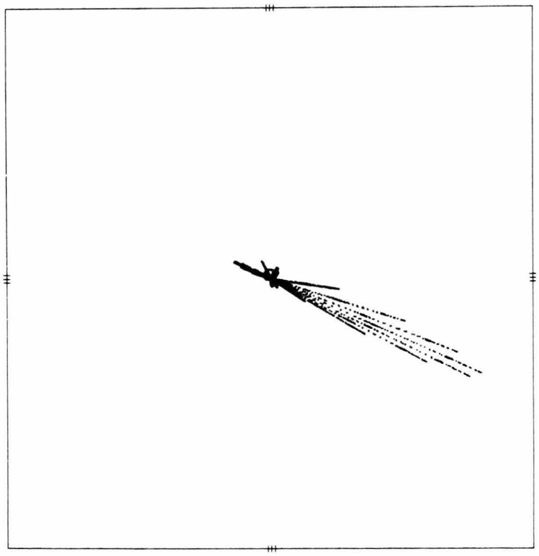

Fig. 15. $P_1(Q_2)$, case H2; $A_1 = 0.5$, $A_2 = -1.76$, $\Delta\alpha = 0.5\,\pi$; $\omega_2 = 0.521111$.
$F_1 = A_1 \times \cos(Q_1) \times \sin(Q_2)$;
$F_2 = A_2 \times \cos(2 \times Q_1) \times \sin(B_2 + Q_2)$.

momenta F_1 and F_2 may change sign, which in the plots corresponds to the crossing of the origin and the ensuing formation of loops, see Figs. 9, 10 and 14. A further increase of max $|F_1|$, max $|F_2|$ yields either an explosiv wealth of very extended loops, see Fig. 11, or a "comet" like structure, Figure 15.

Obviously, in Figs. 11 and 15 the amplitudes are close to some critical values. Beyond the critical values the outcome depends on the class of functions used. For class I functions, to which Figs. 8–11 belong, the critical amplitudes $A_i = A_{ic}$ turn out to be those for which both G_1 and G_2 can change sign.

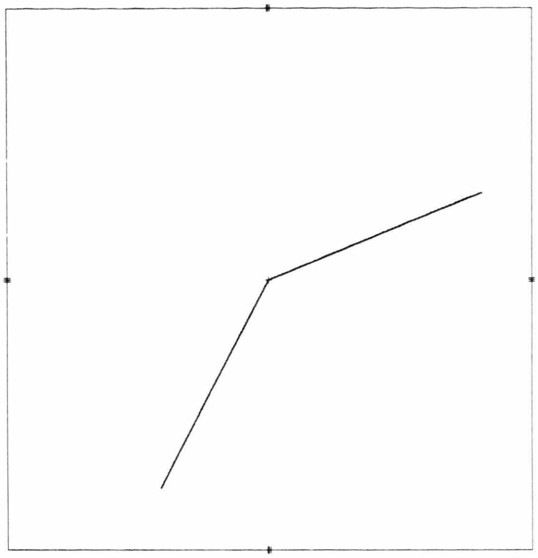

Fig. 16. $P_1(Q_2)$, case H3; $A_1 = 0.5$, $A_2 = 0.3$, $\Delta\alpha = 0.5\,\pi$; $\omega_2 = 0.5$.
$F_1 = A_1 \times \sin(Q_2)$;
$F_2 = A_2 \times \sin(B_2 + 2 \times Q_1)$.

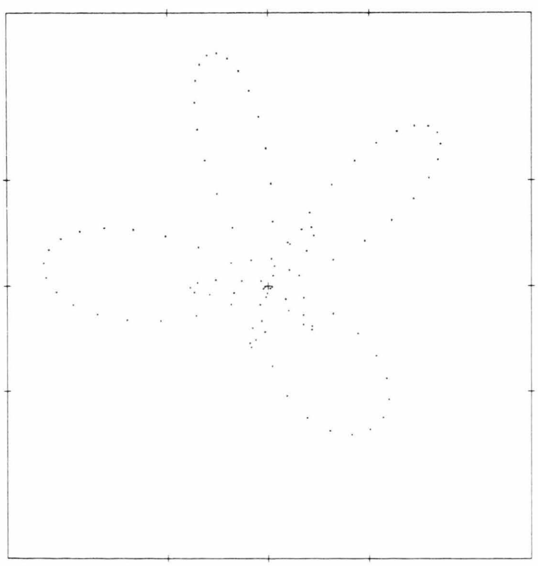

Fig. 17. $P_1(Q_2)$, case H3; $A_1 = 0.5$, $A_2 = 0.3$, $\Delta\alpha = 0.5\,\pi$; $\omega_2 = 51/100$.
$F_1 = A_1 \times \sin(Q_2)$;
$F_2 = A_2 \times \sin(B_2 + 2 \times Q_1)$.

For "supercritical" amplitudes the computational method for the surface of section plots breaks down, as explained above. Computations with the independent variable t show, however, that P_1, P_2 become unstable, i.e. they increase unboundedly with increasing t, if the $Q_2(Q_1)$ orbit is as in Figure 3. For class II Hamiltonians, see Figs. 12–15, the $Q_2(Q_1)$ flow changes at the critical amplitudes A_{ic} from the ergodic to the attracting type, Fig. 6. Here, the A_{ic} are, in general, not related to a change of sign of G_1 or G_2. (In the example in Sect. 3 they are, caused by the particular simplicity of the example.) For "supercritical" amplitudes there is again an instability. The surface of section plots show very few scattered points visible with a reasonable scale of the figures owing to exponential divergence of $|P_i|$.

For class I Hamiltonians with rational $\omega_2/\omega_1 = m/n$ (and $\langle F_i \rangle = 0$) the $Q_2(Q_1)$ flow is also non ergodic, see Figure 4. In this case the surface of section plots usually consists of n sequences of points, each on a line, with $|P_i|$, $i = 1, 2$, growing linearly in time, provided that n is not too large. Figure 16 is an example with $\omega_2/\omega_1 = 1/2$. For large n, however, the surface of section plot changes to a periodic assembly of points. Figure 17 with $\omega_2/\omega_1 = 51/100$ shows exactly 100 points although 1000 points were calculated and plotted. The transition, with the parameters used in Figs. 16 and 17, takes place somewhere between $n = 15$ and $n = 20$. Obviously, any number ω_2/ω_1, such as 0.251111 in Figs. 8–15, used to mimic an irrational number leads to periodicity of the solution with such a long recursion period that ergodicity for $Q_2(Q_1)$ or continuity for P_1 are indeed mimicked.

The functions used in Figs. 10, 11 and 16, 17 are $F_1 = A_1 \sin Q_2$, $F_2 = A_2 \sin(B_2 + 2\,Q_1)$, case H3, and, in Figs. 13, 14, $F_1 = 2\sqrt{2 + \sin Q_1} + A_1 \sin Q_2$, $F_2 = 0.5\,A_2\,[\sin(B_1 + Q_1) + 0.6 \sin(B_2 + Q_2)]^2$, case H4. (Here, as an exception $\langle F_i \rangle \neq 0$.) Class I Hamiltonians which, unlike cases H1, H3, have F_{11}, $F_{22} \neq 0$ show qualitatively the same behaviour as cases with $F_{11} = F_{22} = 0$.

In those cases where $|P_i|$ stays bounded one can Fourier analyze the time evolution $P_i(t)$. Figure 18 shows the spectrum $P_1(\omega)$ for a class I Hamiltonian, case H3, with $A_1 = 0.4$, $A_2 = 1.0$ and $\omega_2 = 0.521111$. The unit frequency is marked on the abscissa. The spectrum consists of lines $\omega_{r,s} = r\,2\,\omega_1 + s\,\omega_2$, with r and s integer. For the most prominent lines r and s are indicated. The spectra of $Q_i^*(t) = Q_i(t) - \omega_i\,t$, $i = 1, 2$, are of the same type. Such quasi-harmonic spectra confirm integrability: The P_i are $2\,\pi$-periodic functions of Q_1, Q_2 and hence of $\omega_1\,t$, $\omega_2\,t$.

With increasing A_1, A_2 the spectra become denser from lines with higher $|r|$, $|s|$. The increasing

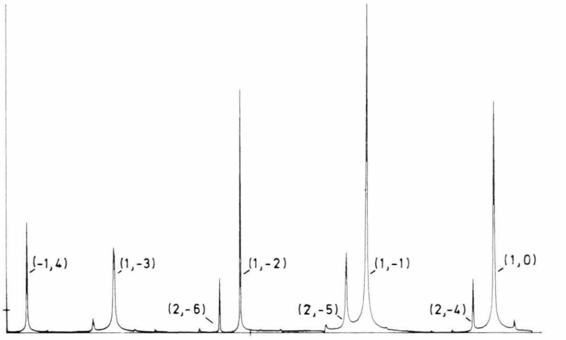

Fig. 18. Spectrum $P_1(\omega)$, case H3; $A_1 = 0.4$, $A_2 = 1.0$, $\Delta\alpha = 0.5\,\pi$; $\omega_2 = 0.521111$.
$F_1 = A_1 \times \sin(Q_2)$;
$F_2 = A_2 \times \sin(B_2 + 2 \times Q_1)$.

density corresponds to the profusion of loops in the corresponding surface of section plots. If the amplitudes are increased so much that, with initial values Q_{10}, Q_{20} in the ergodic region, a flow with changing sign of both G_1 and G_2 is obtained, the spectra seem to become diffuse, see Fig. 19, case H3, with $A_1 = 2.0$, $A_2 = 1.0$, $\omega_2 = 0.521111$. Unfortunately, the demand on computing time rises exponentially in this domain of amplitudes. A stationary state for max $|P_1(t)|$, if it exists, has not yet been reached at $t = 262 \cdot 2\,\pi/\omega_1$ in the sequence of $P_1(t)$, the analysis of which yielded Figure 19. No conclusions on integrability can therefore be drawn from the spectra in this regime.

For class II Hamiltonians with $|P_i|$ bounded the spectra are also found to be harmonic combinations of two fundamental frequencies, say Ω_1 and Ω_2. Here, however, the Ω_i depend on the amplitudes A_1, A_2, with $\Omega_1, \Omega_2 \to \omega_1, \omega_2$ for $A_1, A_2 \to 0$.

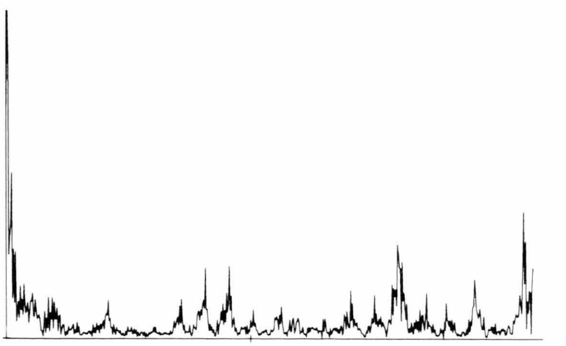

Fig. 19. Spectrum $P_1(\omega)$, case H3; $A_1 = 2.0$, $A_2 = 1.0$, $\Delta\alpha = 0.5\,\pi$; $\omega_2 = 0.521111$.
$F_1 = A_1 \times \sin(Q_2)$;
$F_2 = A_2 \times \sin(B_2 + 2 \times Q_1)$.

3. Theoretical aspects

The unexpected result of the previous section was the fact that no manifestedly non-integrable Hamiltonians were found numerically. One might therefore think that these Hamiltonians are trivally integrable, and might try to find an additional invariant $I(\boldsymbol{P}, \boldsymbol{Q})$ from the partial differential equation

$$[I, H] = \sum_{i=1,2} \left(\frac{\partial I}{\partial Q_i} \frac{\partial H}{\partial P_i} - \frac{\partial I}{\partial P_i} \frac{\partial H}{\partial Q_i} \right) = 0 \,. \quad (3.1)$$

With an ansatz such as

$$I = \sum_{r=0,n} P_1^r P_2^{n-r} I_r(Q_1, Q_2) \quad (3.2)$$

and some trial it is indeed possible to obtain single-valued $2\,\pi$-periodic invariants I for certain more or less simple types of $G_i(Q_1, Q_2)$, $i = 1, 2$.

For example, let c_1, c_2 be arbitrary constants and $h_1(Q_1)$, $g_2(Q_2)$ harmonic functions which satisfy $c_2 h_1''/h_1 = g_2''/g_2 = \text{const.}$ Then, with

$$G_1(Q_1, Q_2) = c_1 + c_2 h_1'(Q_1)\, g_2(Q_2),$$
$$G_2(Q_1, Q_2) = h_1(Q_1)\, g_2'(Q_2), \quad (3.3)$$

where the prime denotes differentiation, a proper invariant is given by

$$I(P_1, P_2, Q_2) = (P_1^2 - c P_2^2)\,[g_2'(Q_2)]^2 \,. \quad (3.4)$$

(It may be noteworthy that it is not possible in general to obtain another invariant $\tilde{I} = \tilde{I}(I, H)$ which is linear in P_1, P_2.)

For general $G_i(Q_1, Q_2)$ it does not seem possible to write explicit expressions for $I(P_1, P_2, Q_1, Q_2)$ if such invariants other than H exist. It seems all the more impossible to decide whether potential invariants are $2\,\pi$-periodic in Q_1, Q_2, as required for integrability. For two classes of Hamiltonians it will be shown that the (dis-) proof of periodicity is indeed a much harder problem than finding an invariant in the first place.

Let us first consider Hamiltonians with div $\boldsymbol{G} = 0$ and, in addition

$$G_{11} = G_{22} = 0 \,, \quad (3.5)$$

as used in H1, H3 of Sect. 2. From (3.5) and (2.1) one obtains

$$G_2(Q_1)\, dQ_1 = G_1(Q_2)\, dQ_2 \,, \quad (3.6)$$

which determines $Q_2(Q_1)$ from the relation

$$\int_{Q_{10}}^{Q_1} dQ_1'\, G_2(Q_1') = \int_{Q_{20}}^{Q_2} dQ_2'\, G_1(Q_2') \,. \quad (3.7)$$

Equations (2.1) for P_1, P_2 may also be solved analytically. (Take Q_1 as "time" variable, for example, eliminate P_2 by an additional differentiation, and note that the resulting second-order equation for P_1 is a total differential.) One obtains

$$P_1(Q_1) = G_2(Q_1)\,[c_1 + c_2 S(Q_1)], \tag{3.8}$$

$$P_2(Q_1) = -G_1(Q_2(Q_1))\,[c_1 + c_2 S(Q_1)] + \frac{c_2}{G_2(Q_1)}$$

with

$$S(Q_1) = \int_{Q_{10}}^{Q_1} \mathrm{d}Q_1' \frac{G_{21}(Q_1')}{G_1(Q_2(Q_1'))\,[G_2(Q_1')]^2}. \tag{3.9}$$

$c_1 = P_{10}/G_2(Q_{10})$ and $c_2 = -H$ are constants of the motion, determined by the values of P_i, Q_i at $t=0$. From (3.8) one immediately obtains the invariant of motion $I = c_1$:

$$I(P_1, P_2, Q_1, Q_2) = \frac{P_1}{G_2(Q_1)} + H(P_1, P_2, Q_1, Q_2)\cdot S(Q_1) \tag{3.10}$$

whose property $[I, H] = 0$ is easily confirmed.

Obviously, for $H = 0$, which can always be achieved for a particular initial direction $\alpha = \alpha_0$ of the vector (P_1, P_2), see Sect. 2, the invariant $I(P_1, Q_1) = P_1/G_2(Q_1)$ is 2π-periodic in Q_1 and the motion is integrable. P_1 is proportional to $G_2(Q_1)$, in agreement with numerical results.

For $H \neq 0$ integrability depends crucially on the properties of $S(Q_1)$. For S 2π-periodic in Q_1 integrability would hold, of course. Considering the fact that the orbit $Q_2(Q_1)$ from (3.7) enters into S, periodicity cannot, however, be expected in general. On the other hand, requiring periodicity in Q_1 is too much. Sufficient for integrability is the requirement that $S(Q_1)$ be represented in the form

$$S(Q_1) = \tilde{S}(Q_1, Q_2) \tag{3.11}$$

with $\tilde{S}$ 2π-periodic in Q_1 and Q_2, with $Q_2 = Q_2(Q_1)$. In Appendix B it is shown that with $\omega_2/\omega_1 = \omega$ the solution of (3.7) is of the form

$$Q_2(Q_1) = \omega Q_1 + \tilde{Q}(Q_1, \omega Q_1) \tag{3.12}$$

with $\tilde{Q}$ 2π-periodic in both arguments and given as a double Fourier series, (B4). In consequence, the integrand in (3.9), denoted by $s(Q_1')$, has the same representation,

$$s(Q_1) = \sum_{m,n=-\infty}^{+\infty} s_{mn}\, \mathrm{e}^{i(mQ_1 + n\omega Q_1)}, \tag{3.13}$$

i.e. it is a quasiperiodic function of Q_1'. From (3.9) it follows that

$$S(Q_1) = s_{00}\cdot(Q_1 - Q_{10}) + \sum_{m,n\neq 0} \frac{s_{mn}}{i(m+n\omega)}\,[\mathrm{e}^{i(mQ_1+n\omega Q_1)} - \mathrm{e}^{i(mQ_{10}+n\omega Q_{10})}]. \tag{3.14}$$

With eqs. (B2, B4) and rearrangement of terms one finally obtains the formal structure

$$S(Q_1) = s_{00}\cdot Q_1 + \sum_{m,n} t_{mn}\,\mathrm{e}^{i(mQ_1+nQ_2)} = s_{00}\cdot Q_1 + \tilde{S}_1(Q_1, Q_2) \tag{3.15}$$

where $\tilde{S}_1$ is 2π-periodic.

In consequence, in order to obtain an invariant (3.10), periodic in Q_1, Q_2, two conditions have to be satisfied: a) the average s_{00} of the integrand in (3.9) has to vanish, and b) all the double m, n series involved in the derivation of (3.15) have to converge.

In all pertinent examples studied in Sect. 2 condition a) was obviously satisfied, except for rational $\omega = \omega_2/\omega_1 = m/n$ with low n, see Figure 16. Apparently, this figure shows the linear increase of P_1, (3.8), resulting from the term $s_{00}Q_1$ in $S(Q_1)$. Hamiltonians of type (3.5) with "low" rational ω_2/ω_1 therefore seem to be non-integrable. For larger n, on the other hand, the observed integrability, see Fig. 17, seems to be real and not an artefact of numerical discretization and round-off errors because improved accuracy does not change the result. The analytic evaluation of s_{00} seems an impossible task, unfortunately, even for G_i as simple as in H3.

The precise formulation of conditions a) and b) requires to distinguish between $\omega = \omega_2/\omega_1$ rational and irrational. For rational ω the double sums are replaced by simple sums and the convergence properties may be discussed relatively easily. For irrational ω, however, there is the classical problem of "small denominators" $m + n\omega \to 0$ for large $|m|$ and $|n|$ in (3.14), which makes the convergence of the series difficult. Analogous convergence problems might exist in the transition from Q_2 to $(Q_1, \omega Q_1)$, see (B2, B4). It is well known [6, 7] that the integral of a quasiperiodic function, say $\tilde{s}(Q_1, \omega Q_1)$, is again a quasiperiodic function only if ω is "sufficiently irrational". Furthermore, $\tilde{s}(Q_1, \omega Q_1)$ must have piecewise continuous h'th order derivatives, with h sufficiently large ($h = 5$ according to [7]).

We have made a deliberate attempt to violate condition b) by using functions G_i whose *first*-order derivatives G_{ij} in (2.2) are only piecewise continuous, namely, case H5, $G_1 = \omega_1 + A_1 f(Q_2)$, $G_2 = \omega_2 + A_2 f(B_2 + 2\,Q_1)$, with

$$f(Q) = \begin{matrix} 2\,Q/\pi - 1 \\ 3 - 2\,Q/\pi \end{matrix} \quad \text{for} \quad \begin{matrix} 0 \leqq Q \leqq \pi \\ \pi \leqq Q \leqq 2\,\pi \end{matrix}, \tag{3.16}$$

and continued periodically. Figure 20 with $A_1 = 0.5$, $A_2 = 0.3$, $\omega_2 = 0.521111$ shows the surface of section plot. It is evident that the attempt to construct a manifestedly non-integrable Hamiltonian by this choice of G_i failed. The only difference to corresponding figures such as Figs. 8–10 is the reduced smoothness of the resulting curve. The observed behaviour is explained if the integrand $s(Q_1)$ in (3.9) is smoother than the functions G_{ij} themselves.

Even for rational ω_2/ω_1 with low m and n there are integrable cases among the Hamiltanions (3.5). Trivial examples are $F_1 = 0$ or $F_2 = 0$ with $I = P_2$ or $I = P_1$ respectively, for all ω_1, ω_2.

For Hamiltonians with compressible flow in $\boldsymbol{Q}$-space, div $\boldsymbol{F} \neq 0$, analogous considerations on integrability as above can again be made for restricted classes of $G_i(Q_1, Q_2)$. For

$$F_2(Q_1, Q_2) = 0 \tag{3.17}$$

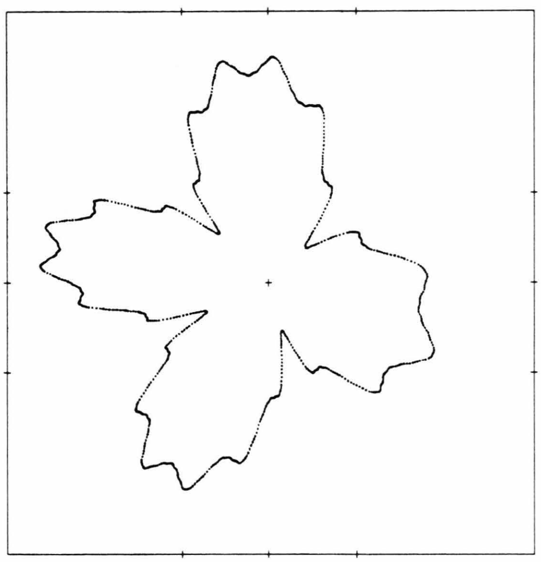

Fig. 20. $P_1(Q_2)$, case H5; $A_1 = 0.5$, $A_2 = 0.3$, $\Delta\alpha = 0.5\,\pi$; $\omega_2 = 0.521111$.
$F_1 = A_1 \times$ 'triangular function' (Q_2),
$F_2 = A_2 \times$ 'triangular function' (Q_1).

for example, one obtains from (2.1)

$$Q_2 = \omega_2\,t + Q_{20}, \tag{3.18a}$$

$$\dot{Q}_1 = \omega_1 + F_1(Q_1, \omega_2\,t + Q_{20}). \tag{3.18b}$$

Substituting the solution $Q_1 = Q_1(Q_2)$ of (3.18b) in (2.2) yields

$$P_1(Q_2) = P_{10} \exp\left\{-\frac{1}{\omega_2}\int_{Q_{20}}^{Q_2} \mathrm{d}Q_2'\,F_{11}(Q_1(Q_2'), Q_2')\right\} \tag{3.19}$$

and similarly for P_2. For the Hamiltonian to be integrable the integral in (3.19), denoted by $T(Q_2)$, must again have a representation of the form $T(Q_2) = \tilde{T}(Q_1, Q_2)$ with $\tilde{T}$ 2π-periodic.

The class (3.17) of G_1, G_2 includes trivially integrable cases with "spectacular" $\boldsymbol{Q}$-flow. A line attractor, for example, is obtained with

$$F_1(Q_1, Q_2) = A_1 \cdot (2\sin^2 Q_1 - 1). \tag{3.20}$$

The solution of (3.18b) is

$$Q_1(t) = \operatorname{arc\,tg}\left\{\frac{\omega_1 - A_1}{\Omega_1}\,\frac{c\exp(2\,\Omega_1\,t) + 1}{c\exp(2\,\Omega_1\,t) - 1}\right\}. \tag{3.21}$$

The effective frequency Ω_1 depends on the amplitude:

$$\Omega_1 = \sqrt{A_1^2 - \omega_1^2}\,. \tag{3.22}$$

It has been assumed that $\Omega_1^2 > 0$, i.e. max $|F_1| > \omega_1$. In the limit $t \to \infty$ Q_1 is attracted to the line $Q_{1\infty} = \operatorname{arc\,tg}[(\omega_1 - A_1)/\Omega_1]$ which implies the limits $G_1 \to 0$ and $P_1(Q_1) = \text{const}/G_1(Q_1) \to \infty$ exponentially fast.

The "Floquet Hamiltonians"

$$F_1(Q_1, Q_2) = A_1\cos^2 Q_1 \cdot f_1(Q_2); \quad F_2 \equiv 0 \tag{3.23}$$

with f_1 arbitrary, 2π-periodic are also of the type (3.17). The canonical transformation $p_1 = \sqrt{2P_1}\sin Q_1$, $q_1 = \sqrt{2P_1}\cos Q_1$ yields the linear differential equation with periodic coefficient

$$\ddot{q}_1 + \omega_1[\omega_1 + f_1(\omega_2\,t)]\,q_1 = 0. \tag{3.24}$$

Floquet theory determines the type of solution $q_1(t)$ [8] and guarantees the existence of an invariant $I(P_1, Q_1, Q_2)$, linear in P_1 and periodic in Q_1, Q_2 although its explicit expression is hard to obtain in general. Linear differential equations with *quasi-periodic* coefficient $f_1(\omega_2 t, \ldots, \omega_n t)$, $n > 2$, are equivalent to non-KAM Hamiltonians with dimension n [5]. The theory of such differential equations is only in its infancy, see [7, 9].

4. Summary and Conclusions

The integrability of non-KAM Hamiltonians was investigated numerically and analytically. Such Hamiltonians are linear in the momenta when the Hamiltonian is expressed in terms of action and angle variables P and Q of the "unperturbed" Hamiltonian.

Many different examples were analyzed. The mixture of islands and stochastic regions typical of KAM Hamiltonians is not observed. Usually, a closed curve is obtained in the surface of section plot, *indicating integrability*, in particular if the "perturbation" part in the Hamiltonian is not too large.

In some cases sequences of points are obtained which go to infinity. Such sequences may be observed with "class I" Hamiltonians (the flow in $\boldsymbol{Q}$ space is divergence-free) if the frequency ratio $\omega_2/\omega_1 = m/n$ is rational with low m, n. For all rational ω_2/ω_1 the flow in $\boldsymbol{Q}$ space reduces to closed lines. For "class II" Hamiltonians (the flow in $\boldsymbol{Q}$ space is compressible) diverging $\boldsymbol{P}$ sequences are observed if the $\boldsymbol{Q}$ flow is attracted to a closed curve or a fixed point. Theoretical considerations suggest that in class I cases the Hamiltonians with diverging $|\boldsymbol{P}|$ are non-integrable, while in class II cases they may still be integrable.

The following partly tentative conclusions can be drawn from these results:

1. The measure of integrable non-KAM Hamiltonians seems to be much higher than that of non-integrable ones, provided the ratio of "perturbation" part to "unperturbed" part in the Hamiltonians is not too large.
2. For non-integrable class I Hamiltonians the momenta $\boldsymbol{P}$ tend to $\pm\infty$. This is not unexpected since the effective frequencies, say Ω_1, Ω_2, in the orbits are independent of the amplitudes of $\boldsymbol{P}$, and resonances are not quenched by nonlinear effects as in KAM Hamiltonians. Resonances are easily constructed since Ω_1, Ω_2 are those of the "unperturbed" Hamiltonian, $\Omega_i = \omega_i$, $i = 1, 2$, and can be chosen at will. Resonances $m\,\Omega_1 = n\,\Omega_2$ with large m, n do not seem to cause non-integrability. In addition, analytic examples exist for which the Hamiltonians are integrable for arbitrary ω_1, ω_2.
3. For class II Hamiltonians the effective frequencies Ω_i are moved away from the "unperturbed" values ω_i by the perturbation part in the Hamiltonian, in spite of its linearity in the momenta. The Ω_i therefore are unknown in practice, except for trivial examples, and resonance $m\,\Omega_1 = n\,\Omega_2$ cannot easily be achived by random variation of parameters. This could explain why (apparently) no non-integrable class II Hamiltonians were observed. Again, Hamiltonians exist which are definitely integrable for arbitrary ω_1, ω_2 and arbitrary amplitude of the "perturbation" term.
4. The distinction between integrable and non-integrable *orbits* for a given non-integrable Hamiltonian which is important in KAM theory disappears almost but not completely for non-KAM Hamiltonians. A class of (apparently) non-integrable Hamiltonians is presented for which all orbits diverge except those with one particular initial direction of the momenta.
5. More fundamental analytic work is required to derive conditions for (non-)integrability. This task is related to the generalization of Floquet's theory and it promises to be as non-trivial as that for KAM Hamiltonians.

Appendix A

We look for canonical transformations $\boldsymbol{P}, \boldsymbol{Q} \rightarrow \boldsymbol{P}', \boldsymbol{Q}'$ where $\boldsymbol{P} = (P_1, \ldots, P_n)$ etc. which transform $H_0(\boldsymbol{P}) = \sum_{i=1,n} \omega_i P_i$ into $\hat{H}_0(\boldsymbol{P}')$, a potentially non-linear function, and retain the 2π-periodicity in $\boldsymbol{Q}'$ of $H_1 = \sum_i P_i F_i(\boldsymbol{Q})$. These specifications are required in order to maintain $\boldsymbol{P}'$ and $\boldsymbol{Q}'$ as action and angle variables. With the generating function $S(\boldsymbol{P}', \boldsymbol{Q})$ we have

$$P_i = \frac{\partial S}{\partial Q_i}; \quad Q_i' = \frac{\partial S}{\partial P_i'}; \quad i = 1, \ldots, n. \tag{A1}$$

The $\boldsymbol{P}$ are functions of $\boldsymbol{P}'$ only, provided

$$S(\boldsymbol{P}', \boldsymbol{Q}) = \sum_{i=1,n} s_i(\boldsymbol{P}') \cdot Q_i. \tag{A2}$$

It follows that

$$Q_i' = \sum_{j=1,n} \frac{\partial s_j}{\partial P_i'} Q_j =: \sum_{j=1,n} \sigma_{ij}(\boldsymbol{P}')\, Q_j \tag{A3}$$

and therefore

$$Q_i = \sum_{j=1,n} (\sigma^{-1})_{ij}\, Q_j', \tag{A4}$$

where σ^{-1} is the inverse of the matrix $\{\sigma_{ij}\}$. Without loss of generality it may be assumed that each of the Q_i, $i = 1, n$, occurs as a variable in at least one of the $F_j(\boldsymbol{Q})$, $j = 1, n$. Otherwise the corresponding P_i would be constant and Hamilton's equations would separate into into a lower-dimensional non-trivial set without P_i, Q_i and a trivial pair of equations for P_i, Q_i. Consequently, the 2-π periodicity of H_1 in Q'_j requires that all elements of σ^{-1} be integers. If, in addition, unsteady transformation $\boldsymbol{P} \to \boldsymbol{P}'$ are excluded, it follows that the elements of σ^{-1} and hence of σ itself are constants, independent of $\boldsymbol{P}'$. From the definition of σ_{ij} one then obtains, apart from trivial constants,

$$s_i = \sum_{j=1,n} P'_j \sigma_{ji} \tag{A5}$$

and from (A1), (A2)

$$P_i = \sum_{j=1,n} P'_j \sigma_{ji}, \tag{A6}$$

so that both $\hat{H}_0(\boldsymbol{P}')$ and the total Hamiltonian $\hat{H}(\boldsymbol{P}', \boldsymbol{Q}') = H(\boldsymbol{P}, \boldsymbol{Q})$ are again linear in $\boldsymbol{P}'$. This proves the genericity of this type of Hamiltonians.

Hamiltonians of type (1.5) are not to be confused with the case called intrinsic degeneracy, where $H_0(\boldsymbol{P})$ is linear and $H_1(\boldsymbol{P}, \boldsymbol{Q})$ is nonlinear in $\boldsymbol{P}$. Here a suitable $\boldsymbol{Q}$-averaged part of H_1 can be added to H_0, so that a new nonlinear $\tilde{H}_0(\boldsymbol{P})$ is obtained, and KAM theory can be applied. See, for example, [10].

Appendix B

From (3.7), $G_i = \omega_i + F_i$ and $\langle F_i \rangle = 0$ one obtains

$$Q_2 = \omega\, Q_1 + \Gamma(Q_1, Q_2), \tag{B1}$$

where Γ is 2 π-periodic. With the ansatz

$$Q_2 = \omega\, Q_1 + \Psi \tag{B2}$$

one gets

$$\Psi = \Gamma(Q_1, \omega\, Q_1 + \Psi). \tag{B3}$$

This determines Ψ as a function $\tilde{Q}(Q_1, \omega\, Q_1)$ which is also 2 π-periodic in both arguments. It has therefore the Fourier representation

$$\Psi = \tilde{Q}(Q_1, \omega\, Q_1) = \sum_{m,n=-\infty}^{+\infty} Q_{mn}\, \mathrm{e}^{i(m Q_1 + n \omega Q_1)}. \tag{B4}$$

[1] L. A. Pars, A Treatise on Analytical Dynamics, Heinemann, London 1965.
[2] M. V. Berry, in: Topics in Nonlinear Dynamics, Ed. Siebe Jorna, American Institute of Physics, New York 1978.
[3] V. I. Arnold, Russian Math. Surveys **18,** 9 (1963).
[4] A. Salat and J. Tataronis, in: Long Time Prediction in Dynamics (C. W. Horton, Jr., L. E. Reichl, and A. G. Szebehely, eds.), John Wiley, New York 1983.
[5] A. Salat, Z. Naturforsch. **37 a,** 830 (1982).
[6] J. Moser, SIAM Review **8,** 145 (1966).
[7] H. Haken, Advanced Synergetics, Springer, Berlin 1983.
[8] V. A. Yakubovitch and V. M. Starzhinskii, Linear Differential Equations with Periodic Coefficients, John Wiley, New York 1975.
[9] N. N. Bogoljubov, Ju. A. Mitropolskii, and A. M. Samoilenko, Methods of Accelerated Convergence in Nonlinear Mechanics, Springer, Berlin 1976.
[10] A. J. Lichtenberg, in: Stochastic Behaviour in Classical and Quantum Hamiltonian Systems (G. Casati and J. Ford, eds.), Springer, Berlin 1979.
[11] A. R. Bishop and T. Schneider, Solitons and Condensed Matter Physics, Springer, Berlin 1978.